BBA - Bioenergetics 1860 (2019) 618–627

Contents lists available at ScienceDirect

BBA - Bioenergetics

journal homepage: www.elsevier.com/locate/bbabio

# Mitochondrial respirasome works as a single unit and the cross-talk between complexes I, $III_2$ and IV stimulates NADH dehydrogenase activity

Reyes-Galindo Meztli[1], Suarez Roselia[1], Esparza-Perusquía Mercedes, de Lira-Sánchez Jaime, Pardo J. Pablo, Martínez Federico, Flores-Herrera Oscar*

*Departamento de Bioquímica, Facultad de Medicina, Universidad Nacional Autónoma de México, 04510 México City, México*

ARTICLE INFO

*Keywords:*
Respirasome
Mitochondrial supercomplexes
Complex I activity
*Ustilago maydis* mitochondria
ROS production

ABSTRACT

*Ustilago maydis* is an aerobic basidiomycete that depends on oxidative phosphorylation for its ATP supply, pointing to the mitochondrion as a key player in its energy metabolism. Mitochondrial respiratory complexes I, $III_2$, and IV occur in supramolecular structures named respirasome. In this work, we characterized the subunit composition and the kinetics of NADH:Q oxidoreductase activity of the digitonine-solubilized respirasome (1600 kDa) and the free-complex I (990 kDa). In the presence of 2,6-dimethoxy-1,4-benzoquinone (DBQ) and cytochrome *c*, both the respirasome NADH:$O_2$ and the NADH:DBQ oxidoreductase activities were inhibited by rotenone, antimycin A or cyanide. A value of 2.4 for the NADH oxidized/oxygen reduced ratio was determined for the respirasome activity, while ROS production was less than 0.001% of the oxygen consumption rate. Analysis of the NADH:DBQ oxidoreductase activity showed that respirasome was 3-times more active and showed higher affinity than free-complex I. The results suggest that the contacts between complexes I, $III_2$ and IV in the respirasome increase the catalytic efficiency of complex I and regulate its activity to prevent ROS production.

## 1. Introduction

The proton electrochemical potential, $\Delta\mu_{H+}$, across energy transducing membranes is the basis of the chemiosmotic hypothesis for energy coupling [1–3]. In mitochondria this electrochemical potential is used for heat production, ion and substrate transport, ATP/ADP exchange, and especially ATP synthesis [4]. The proton translocation across inner mitochondrial membrane occurs through three protein complexes termed NADH:coenzyme Q oxidoreductase (complex I), coenzyme Q:cytochrome *c* oxidoreductase (complex $III_2$, which is a functional dimer), and cytochrome *c* oxidase (complex IV); additionally, the succinate:coenzyme Q oxidoreductase (complex II), that belongs to the electron transport chain, doesn't translocate protons but produce ubiquinol which is a mobile lipid electron carrier [4].

Three models have been proposed to explain the organization of the electron transport chain complexes: 1) “Random collision model”, proposed by Hackenbrock et al. [5] in which individual respiratory complexes in the inner membrane diffuse freely, and electron transfer is based on random collisions between complexes and two small electron carriers, coenzyme Q and cytochrome *c*; 2) “Solid state model”, in which complexes are attached in supra-structures called supercomplexes [6], which have been founded in mitochondria from mammals, plants, fungi, and bacteria; and 3) “Plasticity model”, which involves both previous models [7].

Supercomplexes have a wide distribution in the natural kingdoms, from bacteria to plants and animals. In *Paracoccus denitrificans* the supercomplexes $III_2$:$IV_1$ [8] and $I_1$:$III_2$:$IV_1$ have been reported [9]; while in *Saccharomyces cerevisiae* complex $III_2$ could be attached to one ($III_2$:$IV_1$) or two ($III_2$:$IV_2$) monomers of complex IV [10,11]. In *Neurospora crassa* supercomplexes are composed of complexes I, $III_2$, and IV in different proportions [12]. Supercomplex $I_1$:$III_2$ is the most abundant in potato (*Solanum tuberosum*), bean (*Phaseolus vulgaris*), barley (*Hordeum vulgare*), and *Arabidopsis thaliana* [13–15]. Bovine heart mitochondrial supercomplexes described are $I_1$:$III_2$:$IV_1$, $I_1III_2$, and $III_2IV_1$ [16]. If complexes I, $III_2$ and IV are present in the supercomplex and NADH oxidation and oxygen reduction occur, they are called respirasome [10].

Actually, the architecture of respirasomes from porcine (*Sus scrofa*) heart mitochondria [17] and ovine (*Ovis aries*) heart mitochondria [18] has been determined by cryo-electron microscopy with a resolution of

* Corresponding author at: Departamento de Bioquímica, Facultad de Medicina, Universidad Nacional Autónoma de México, Apdo. Postal 70-159, Coyoacán, 04510 México, Cd. Mx., México.
*E-mail address:* oflores@bq.unam.mx (O. Flores-Herrera).
[1] M. Reyes-Galindo and R. Suarez contributed equally to this paper.

https://doi.org/10.1016/j.bbabio.2019.06.017
Received 1 November 2018; Received in revised form 20 June 2019; Accepted 22 June 2019
Available online 25 June 2019
0005-2728/ 

5.4 Å and 5.8 Å, respectively.

Initially, respirasomes were associated with electron channeling from NADH to oxygen and the enhancement of electron flow between complexes [5,19]; however this hypothesis has been challenged by new structural and functional evidence [17,18,20]. Currently, the accepted role is related to structural stabilization of complex I [6,21], and prevention of oxygen radicals production [7,21–28]. However, the precise role of supercomplexes remains to be defined.

In this work, digitonin-solubilized respirasomes from *Ustilago maydis* mitochondria were isolated and their subunit composition and activity were characterized. *U. maydis* is an aerobic basidiomycete which infects the corn and teocinte plants in a biotrophic way [29]. In the laboratory the non-pathogenic yeast form of *U. maydis* is easily maintained in standard growth conditions [30]. *U. maydis* contains the four classic mitochondrial respiratory complexes and depends on the oxidative phosphorylation for the supply of ATP [31]. Supercomplexes isolated from *U. maydis* contained complexes I, $III_2$ and IV, as well as coenzyme Q and cytochrome *c*. NADH oxidation supported oxygen uptake and was sensitive to KCN, antimycin A or rotenone. Additionally, complex I activity from respirasome was inhibited by antimycin A or KCN, even upon the addition of coenzyme Q and cytochrome *c*, suggesting a tight functional interaction between complexes. Kinetic characterization of NADH:Q oxidoreductase activity showed that respirasome was 3-times more active than free-complex I, suggesting a stimulatory effect of the contacts between complexes in the respirasome.

## 2. Materials and methods

### 2.1. Cell culture and mitochondria isolation

*U. maydis* cells (strain FB2) were prepared as previously described [31]. *U. maydis* mitochondria were isolated using the method described by Waterfield and Sisler [32]. For details see Supplemental material.

### 2.2. Solubilization of respiratory supercomplexes

The respiratory supercomplexes and complexes were solubilized from *U. maydis* mitochondria using digitonin (a very-mild detergent) as described by [33–35], with minor modifications [36]. Briefly, *U. maydis* mitochondria (10 mg/ml) were suspended in 3.5 ml of 50 mM Bis-Tris and 500 mM 6-aminocaproic acid, pH 7.0 and 140 µl digitonin (50% stock) were added to reach a detergent/protein ratio of 2:1. Digitonin was added drop by drop while the mixture was gentle stirred in an ice bath and then incubated in this condition during 30 min. The mixture was centrifuged at 100,000*g* for 30 min at 4 °C and supernatant containing the supercomplexes and individual complexes was recovered and immediately loaded into a sucrose gradient (16–42%) for supercomplexes isolation (*vide infra*).

### 2.3. Respirasome isolation

Mitochondrial digitonin extract (16 mg protein) was loaded on 24 ml of a continuous sucrose gradient (16–42% sucrose, 15 mM Tris, pH 7.4, 20 mM KCl and 0.2% digitonin) and centrifuged at 131,000*g* for 16 h at 4 °C [36]. Afterward, 500 µl fractions were collected from the bottom of the gradient. Fractions containing respirasomes were identified by BN-PAGE (*vide infra*). These respirasomes samples were pooled and diluted 7-fold with 30 mM HEPES, pH 8.0 and 5% glycerol; then were concentrated using a Centrifugal Filters Units (100K, Millipore Amicon Utra) to a final volume of 100 µl, and stored at –70 °C until used.

### 2.4. Blue Native-PAGE and in-gel catalytic activity assays

Samples from the sucrose gradient and the later supercomplexes fraction were loaded on a linear polyacrylamide gradient gel (4–10%) for Blue Native PAGE (BN-PAGE) [35]. The BN-PAGE buffers were 50 mM Bis-Tris/HCl, pH 7.0 for the anode electrode, and 50 mM tricine, 15 mM Bis-Tris, pH 7.0 and the anionic Coomassie© Brilliant Blue R-125 dye (0.02%) for the cathode electrode [35]. The voltage was set to 35 V for 10 h at 4 °C and the run was stopped when the sharp line of the dye approached the gel front. Molecular weight of the respiratory complexes and supercomplexes was determined by their electrophoretic mobility and in-gel catalytic activity, using the complexes of digitonine-solubilized bovine heart mitochondria as standards.

The in-gel assays were performed as described by Jung [34] using gel loaded with isolated digitonine-solubilized supercomplexes from of *U. maydis* mitochondria. NADH dehydrogenase activity (NADH:-methylthiazolyldiphenyl tetrazolium bromide (MTT) oxidoreductase) was assayed at 20–25 °C in a buffer containing 1.2 mM MTT and 1.0 mM NADH in 10 mM Tris/HCl, pH 7.4. For succinate dehydrogenase activity (Succinate:MTT oxidoreductase) NADH was replaced by 10 mM succinate, 0.2 mM phenazine methosulfate (PMS), 5 mM EDTA in 10 mM $K_2HPO_4$, pH 7.4. NADH or succinate dehydrogenase activity was correlated with the development of purple precipitates on the gel. When activity-staining appear (10–20 min) the reaction was stopped with fixing solution (50% methanol, 10% acetic acid). To assay the activity of complex IV the gel was incubated in 50 mM $K_2HPO_4$, pH 7.2, 4.7 mM 3,3′diaminobenzidine tetrahydrochloride (DAB) and 16 µM horse heart cytochrome *c*. After 30–40 min of incubation at 20–25 °C, the activity was observed as a brown precipitate and the reaction was stopped with the fixing solution. Activity of complex V was assayed in 50 mM glycine (adjusted to pH 8.0 with triethanolamine), 10 mM $MgCl_2$, 0.15% Pb $(ClO_4)_2$ and 5 mM ATP. ATP hydrolysis correlated with the development of white lead phosphate precipitates. The reaction was stopped using 50% methanol, and subsequently the gel was transferred to water and scanned against a dark background as described previously [36,37].

### 2.5. Kinetic characterization of NADH dehydrogenase activity from respirasomes and free-complex

Activity of complex I (NADH:2,6-dimethoxy-1,4-benzoquinone (DBQ) oxidoreductase activity) from respirasomes or free-complex I was determined spectrophotometrically at 340 nm by following the oxidation of NADH ($\varepsilon_{NADH} = 6.22\ mM^{-1}\ cm^{-1}$) in an Agilent 8453 UV–visible spectrophotometer (Agilent Technologies, USA). Activity of isolated respirasomes or free-complex I was performed in a reaction mixture containing 120 mM KCl, 5 mM $MgCl_2$, 1 mM EGTA, 30 mM $KH_2PO_4$, pH 7.4, at 25 °C. Where indicated, isolated respirasomes or free-complex I, were added to the buffer described above plus 10 µM of horse heart cytochrome *c* [38], 10–1000 µM of DBQ and 10–150 µM NADH to start the reaction. Where indicated, rotenone (1–10 µM) [39–41], antimycin A (0.1–1 µM) [42–44], or cyanide (1–3 mM) [45,46] were added. Addition of cyanide increased the pH to 7.8, but the activity of complex I and the respirasome was the same at pH 7.4 and pH 7.8 (data no shown). To explore the effect of phospholipids on the activity of free-complex I and respirasomes, the protocol reported by [47] was followed using asolectin or lecithin.

Protein concentration of respirasome or free-complex I was 50 µg/ml and the reaction was started by the addition of NADH. NADH absorbance was continuously monitored and the time response was less than 1 s. Kinetic analysis of changes in NADH dehydrogenase activity (initial velocity) was carried out using the direct spectrophotometric recording. Initial velocities were further obtained from the slope of the linear region in each spectrophotometric recording, and the linear region of the traces was corroborated with the plot of the first derivative against time. Data were analyzed by robust, weighted, non-linear regression analysis using the SigmaPlot software (Systat Software, Inc., version 10.0). The data represent the average of eight independent experiments. Rotenone was added to inhibit NADH:DBQ

**Table 1**
Subunit identity and molecular mass of *Ustilago maydis* mitochondrial respirasomes. The identity of each subunit was determined by LC/ESI-MS/MS.

| Subunit identity | MW mature protein (kDa) | Exclusive unique peptides | Unique exclusive spectra/total spectra | Coverage (%) | ID (Scaffold-NCBI) | ID (KEGG/PENDANT) |
|---|---|---|---|---|---|---|
| | | | Complex I | | | |
| NUAM | 77.2 | 33 | 51/103 | 53 | Q4P4Z1 | UMAG_10695 |
| NUBM | 51.6 | 18 | 20/32 | 31 | Q4PGP5 | UMAG_11170 |
| NUCM | 48.2 | 17 | 27/47 | 45 | Q4P4N9 | UMAG_11162 |
| NUGM | 28.3 | 8 | 13/18 | 21 | Q4PDY2 | UMAG_11896 |
| NUHM | 24.3 | 7 | 8/15 | 32 | Q4PGX9 | UMAG_00634 |
| NUKM | 20.5 | 5 | 9/18 | 26 | Q4P1W1 | UMAG_11038 |
| NUFM | 13.4 | 5 | 7/15 | 51 | Q4P7I2 | UMAG_11517 |
| NB4M | 15.0 | 3 | 4/4 | 31 | Q4PBS6 | UMAG_02437 |
| NUPM | 17.2 | 4 | 6/8 | 44 | | UMAG_05598 |
| NUEM | 35.1 | 17 | 23/40 | 57 | Q4PHN2 | UMAG_00381 |
| N7BM | 14.1 | 5 | 6/11 | 41 | Q4P6C6 | UMAG_10847 |
| NI2M | 10.1 | 4 | 5/8 | 38 | Q4P2N8 | UMAG_05625 |
| NUYM | 17.2 | 6 | 10/16 | 34 | Q4PHA1 | UMAG_00512 |
| NUJM | 14.1 | 4 | 4/7 | 55 | Q4PAH0 | UMAG_11495 |
| NUXM | 20.9 | 5 | 8/11 | 46 | Q4P5K7 | UMAG_10989 |
| NUZM | 22.2 | 5 | 8/21 | 40 | Q4P0U1 | UMAG_12039 |
| NB6M | 10.7 | 5 | 6/14 | 52 | Q4PF02 | UMAG_01311 |
| | | | Complex $III_2$ | | | |
| QCR2 | 43.2 | 17 | 27/49 | 56 | Q4PEI5 | UMAG_01478 |
| Cyt1 | 30.4 | 10 | 15/29 | 36 | Q4P5I2 | UMAG_11534 |
| QCR7 | 10.5 | 8 | 11/14 | 70 | Q4P6M6 | UMAG_04237 |
| RIP1 | 26.5 | 6 | 9/22 | 21 | Q4P7T8 | UMAG_10507 |
| | | | Complex IV | | | |
| Cox2 | 28.6 | 5 | 8/14 | 30 | Q0H8Y7 | Q0H8Y7 |
| Cox4 | 12.8 | 3 | 4/9 | 41 | Q4P511 | UMAG_04802 |
| Cox5A | 16.8 | 7 | 10/20 | 46 | Q4P348 | UMAG_05465 |
| | | | Cytochrome *c* | | | |
| | 11.9 | 3 | 4/7 | 39 | XP_011389077 | UMAG_02708 |

The identity of each protein was determined by mass spectrometry. The subunit molecular weight of the mature protein was determined by 2D-Tricine-SDS-PAGE and corroborated with the molecular weight obtained from *U. maydis* genome analysis (Biomax informatics ag; http://pedant.helmholtz-muenchen.de/pedant3htmlview/pedant3view?Method=analysis&Db=p3_t237631_Ust_maydi_v2GB).

oxidoreductase activity of complex I; samples used in this work were 100% inhibited by rotenone, confirming that complex I was the only NADH dehydrogenase present in both samples. The concentration of complex I in respirasome and free-complex I samples was determined by a densitometry analysis of Coomassie© Brilliant Blue R-125 stained NUAM 77 kDa-subunits (ID Scaffold-NCBI Q4P4Z1; ID KEGG/PENDANT UMAG_10695, Table 1) from an SDS-Tricine-PAGE, using Coomassie stained BSA as a standard (see Supplemental material section). The gel was scanned and the stain-intensity of NUAM subunit and BSA was determined by the Image Analysis software version 1.0 (Thermo Fisher Scientific Inc.). The intensities of NUAM subunit and BSA were measured by peak integration after densitometry analyses. The mol of NUAM subunit was determined using the molecular weight of the mature protein (Table 1). The amount of complex I in respirasomes and free-complex I samples was 3.3 ± 0.7 μg/10 μg total protein and 2.8 ± 0.5 μg/10 μg total protein, respectively; these amounts of complex I in respirasomes and free-complex I were used to kinetics parameters estimation.

### 2.6. Oxygen consumption by mitochondrial respirasomes

Oxygen consumption by isolated respirasomes was determined using a type Clark electrode in the buffer described above at 30 °C. Mixture reaction was supplemented with 10 μM horse heart cytochrome *c*, 70 μM DBQ and 20–100 μM NADH. Maximum activity of complex IV from respirasomes was assayed with 4 mM ascorbate and 6 mM 2,3,5,6-tetramethyl-*p*-phenylendiamine (TMPD) to reduce the horse heart cytochrome *c*. Where indicated, rotenone (10 μM), antimycin A (1 μM), or cyanide (3 mM) were added.

### 2.7. Quantification of hydrogen peroxide produced by respirasomes

Quantification of hydrogen peroxide was performed with Amplex® Red hydrogen peroxide assay kit (Invitrogen, Molecular Probes, USA), following the manufacturer instructions. Experimental conditions used were similar to those described in Section 2.5 (*vide supra*). Superoxide dismutase (50 U/ml) was added to the reaction mixture to accelerate the production of hydrogen peroxide from the superoxide anion.

### 2.8. Tandem mass spectrometry (LC/ESI–MS/MS)

Protein identification of isolated supercomplexes was determined by mass spectrometry performed by the Arizona Proteomics Consortium (Cancer Center and by the BIO5 Institute of the University of Arizona). Samples were prepared following the specifications of the Proteomics Core Laboratory. Scaffold program (version Scaffold_4.8.9, Proteome Software Inc., Portland, OR) was used to validate MS/MS based peptide and protein identifications. Peptide identifications were accepted if they could be established at greater than 95.0% probability by the Scaffold Local FDR algorithm. Protein identifications were accepted if they could be established at greater than 99.0% probability and contained at least 2 identified peptides. Protein probabilities were assigned by the Protein Prophet algorithm [48]. Proteins that contained similar peptides and could not be differentiated based on MS/MS analysis alone were grouped to satisfy the principles of parsimony. Proteins sharing significant peptide evidence were grouped into clusters. Proteins were annotated with GO terms from NCBI (downloaded Apr 24, 2018) [49].

### 2.9. Determination of protein concentration

Samples were treated with 0.4% deoxycholate and the protein content was determined as described by Lowry et al. [50]. Bovine

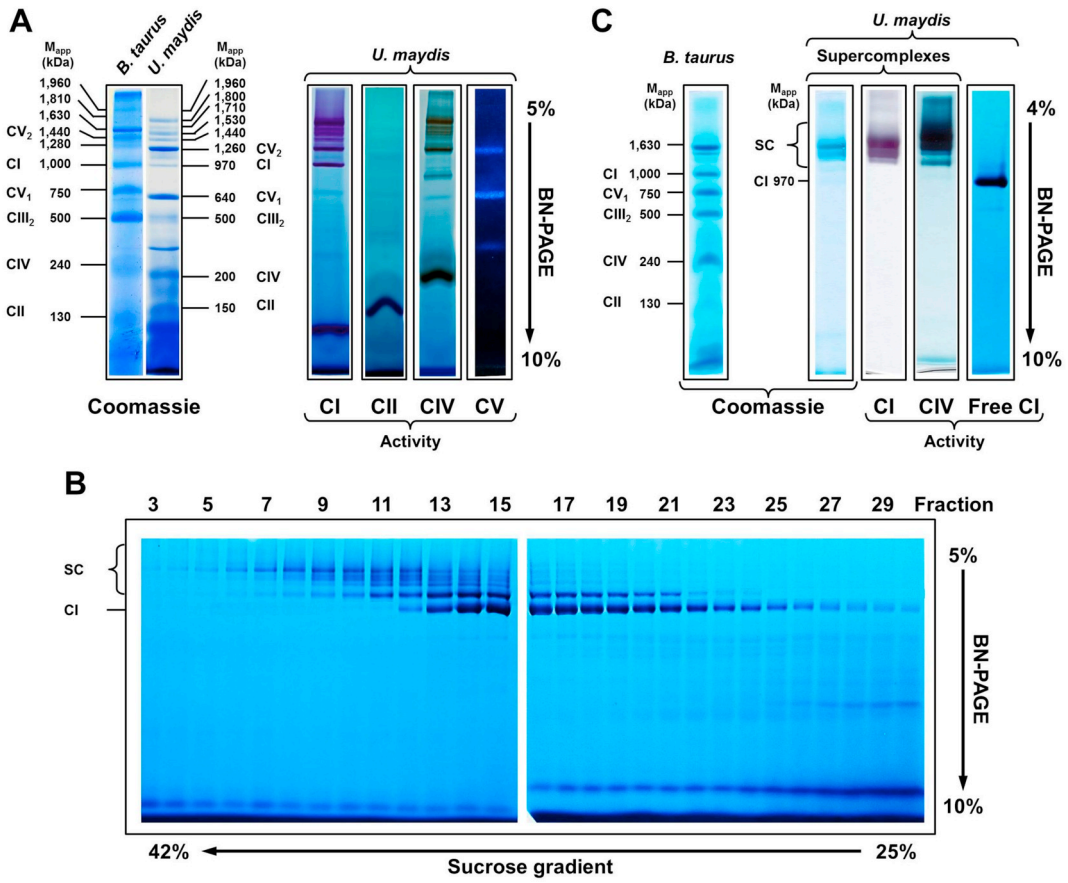


**Fig. 1.** Isolation and in-gel activity of the respirasome. Respiratory complex and supercomplexes from *U. maydis* mitochondria were solubilized with digitonin (A). Left panel shows the Coomassie-stained native gel strips; CI, CII, CIV, and CV corresponding to in-gel activities assay of complexes I, II, IV, and V, respectively. Respirasome was isolated by sucrose-gradient ultracentrifugation and its in-gel NADH dehydrogenase activity analyzed by BN-PAGE (B). Fractions from the bottom [3–11] and the top [25–30] of the sucrose gradient were used to obtain isolated the respirasome and free-complex I, respectively (C). Where is showed *Bos taurus* respiratory complex and supercomplexes were solubilized with digitonin and used as standard. *U. maydis* respirasome sample was used to subunits identification by MS/MS (Table 1).

serum albumin (BSA) was used as standard.

### 2.10. Materials

Analytical grade reagents were purchased from Sigma Chemical Co. (St. Louis, MO, USA), E. Merck (Darmstadt, Germany), and BioRad (Hercules, CA, USA). Strain FB2 of *U. maydis* was obtained from the American Type Cell Collection (Manassas, VA, USA).

## 3. Results

### 3.1. Composition of isolated respirasomes

Respiratory complexes and supercomplexes from *U. maydis* mitochondria were efficiently solubilized with digitonin preserving their activity (Fig. 1A). In gel-activity of individual complex I, II, IV and V was associated with a protein band of a molecular mass of 960, 150, 240 and 640 kDa, respectively; additionally, ATPase activity of complex V was associated with a single protein band of 1260 kDa, which has been reported as the dimer of $F_1F_0$-ATP synthase [36]. Activities of complexes I and IV were associated with several bands with molecular masses from 1400 to 1900 kDa (Fig. 1A). MS/MS analysis confirmed the presence of complex $III_2$ in these supercomplexes.

Digitonin-solubilized respirasomes from *U. maydis* were isolated by sucrose density gradient centrifugation (Fig. 1B). NADH:MTT oxidoreductase activity from complex I was distributed from fraction 3 to 30; however, fractions 3–11 contained exclusively the respirasome, and this pattern was highly reproducible (Fig. 1B). Free-complex I was recovered from fractions 25–30. The fractions containing respirasomes and free-complex I were pooled separately and concentrated as described in the Materials and methods section and their purity, in terms of NADH dehydrogenase activity, was analyzed by BN-PAGE (Fig. 1C). For the respirasomes, activities of complex I and IV were associated with a main protein band of 1600 kDa, using bovine mitochondrial respiratory complexes solubilized with digitonin as standard (Fig. 1C). No activity of monomeric complex I and IV, or complex $III_2$ stained with Coomassie was observed, demonstrating that supercomplexes were isolated without contamination by individual complexes. Free-complex I activity was located around 970 kDa as a single band (Fig. 1C, right lane).

Although activities of complexes I and IV were observed in the upper zone of the gel (Fig. 1B), suggesting a broad spectrum of supercomplexes stoichiometries, a main protein band of 1630 kDa was observed in the gel stained with Coomassie (Fig. 1C). Using the molecular weight obtained from *U. maydis* genome database (Biomax informatics ag; http://pedant.helmholtz-muenchen.de/pedant3htmlview/pedant3view?Method=analysis&Db=p3_t237631_Ust_maydi_v2GB) for complex I (900 kDa), dimer of complex $III_2$ (473 kDa), and complex IV (203 kDa), we hypothesize that the minimum and most probable stoichiometry of this 1630 kDa supercomplex is $I_1$:$(III_2)_1$:$IV_1$. Seventeen subunits for complex I, 4 subunits for complex $III_2$, and 3 for complex IV were identified by MS/MS analysis of isolated respirasomes (Table 1), confirming their composition. Additionally, cytochrome *c* was detected in the respirasome

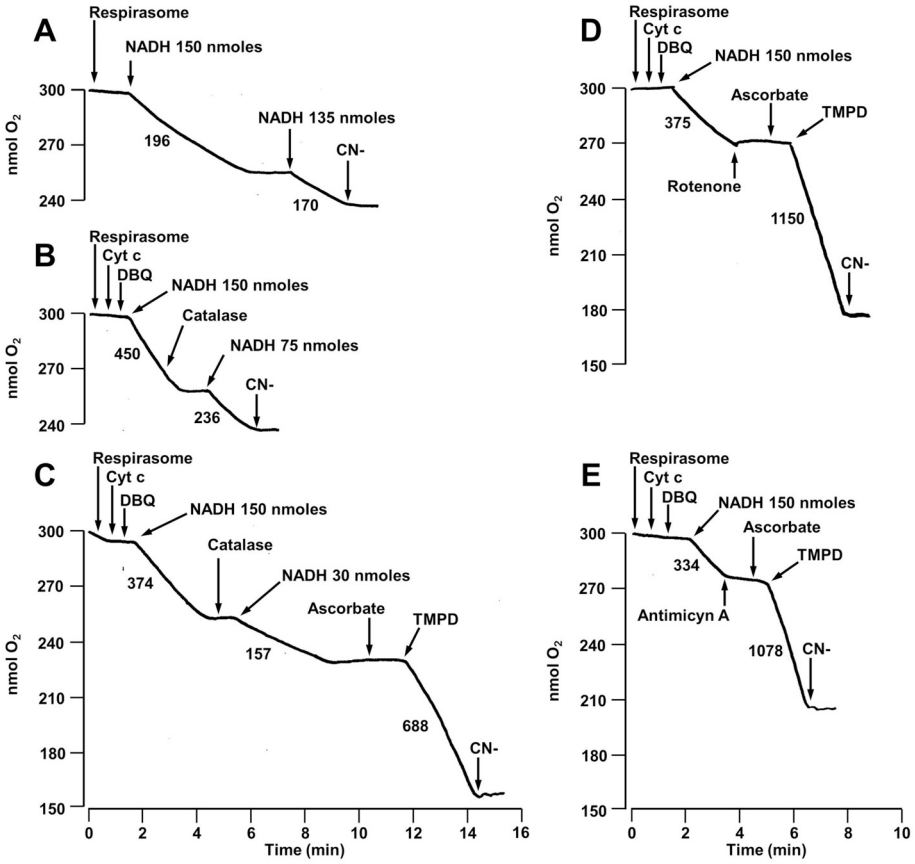


**Fig. 2.** Oxygen consumption by isolated *Ustilago maydis* respirasome. (A) Electron flux into respirasome was started by 150 nmol of NADH addition in 120 mM KCl, 5 mM $MgCl_2$, 1 mM EGTA, 30 mM $KH_2PO_4$, pH 7.4, at 30 °C. (B) Mobile electron carriers stimulate respirasome oxygen uptake (*i.e.* 65 μM DBQ and 60 μg cytochrome *c*/ml). Maximum activity of complex IV was reached by ascorbate (4 mM) and TMPD (6 mM) addition (C). Where is showed 15 μM rotenone (D), 3 μM antimycin A (E) or 3 mM cyanide (A–E) were added to inhibit respiration through complexes I, $III_2$ or IV, respectively. Catalase = 2000–4000 Units. Numbers below each recording represent the velocity of oxygen consumption = nmol $O_2$/mg of CI·min. Different NADH concentrations were added to assay the respirasomes response and the oxygen reduction mean ± S.D. was: 133 ± 17 nmol $O_2$ reduced/mg of CI·min with 30 nmol of NADH added (n = 6); 266 ± 30 nmol $O_2$ reduced/mg of CI·min with 75 nmol of NADH added (n = 6); and 397 ± 81 nmol $O_2$ reduced/mg of CI·min with 150 nmol of NADH added (n = 10). The x-axis scale showed at bottom of C and E is the same for the upper recording (A, B and D). Results were obtained from 7 different preparations.

sample (Table 1). Complex I amount was determined as described in Materials and methods section and Supplementary material.

### 3.2. Oxygen consumption by respirasomes

Surprisingly, isolated respirasomes reduced oxygen in the presence of NADH (133 ± 17 nmol $O_2$ reduced·(mg of CI·min)$^{-1}$), suggesting that they contain, in addition to functional respiratory complexes I, $III_2$ and IV, the mobile elements, coenzyme Q and cytochrome *c*, allowing the electron flux from NADH to oxygen (Fig. 2A). If mobile electron carriers (*i.e.* 60 μg cytochrome *c*/ml and 65 μM DBQ) were added to the reaction mixture, oxygen consumption increased (397 ± 41 nmol $O_2$ reduced·(mg of CI·min)$^{-1}$; Fig. 2B–E), suggesting that these could be used as substrates by isolated respirasomes. Once NADH has been oxidized, oxygen uptake decreases (Fig. 2A–C), and a new NADH addition promoted respiration again. Although oxygen uptake was supported by NADH oxidation, the maximum complex IV activity was reached with ascorbate and TMPD addition (992 ± 203 nmol $O_2$ reduced·(mg of CI·min)$^{-1}$; Fig. 2C–E), indicating that flux control could belong to complexes I or $III_2$. Oxygen reduction by respirasome in the presence of NADH, cytochrome *c* and DBQ was inhibited by rotenone (Fig. 2D), antimycin A (Fig. 2E), or cyanide (Fig. 2A–E). The total inhibition of electron flux by these specific inhibitors discards the presence of rotenone-insensitive alternative NADH dehydrogenases (*i.e.* Nde1, Nde2, or Ndi1) or cyanide-resistant alternative oxidase [31] in isolated respirasomes. Additionally, MS/MS analysis confirms the absence of these alternative respiratory elements in the *U. maydis* respirasome. The absence of hydrogen peroxide ($H_2O_2$) as a result of electron leak during NADH oxidation was demonstrated by the addition of catalase (Fig. 2A and B). Alternatively, $H_2O_2$ production by respirasomes, assayed with the Amplex Red probe, was of 240 ± 4 pmol of $H_2O_2$·(mg of CI·min)$^{-1}$ in the presence of 150 nmol of NADH to assess the maximum rate of oxygen consumption; Cyanide addition increased ROS production to 550 ± 10 pmol of $H_2O_2$·(mg of CI·min)$^{-1}$, and 484 ± 24 pmol of $H_2O_2$·(mg of CI·min)$^{-1}$ in the absence or presence of superoxide dismutase, respectively. These values represent 0.001% of the maximum rate of oxygen consumption supported by NADH.

Since $H_2O_2$ production was negligible (*i.e.* less than 0.001%) during maximum oxygen consumption by respirasome, one question is arising, the NADH:DBQ oxido-reductase activity of complex I occur even if electron flow in complex $III_2$ and IV in supercomplexes is interrupted by antimycin A or cyanide? To answer this question, NADH:DBQ oxido-reductase activity by respirasomes was monitored in the presence of inhibitors of complex I, $III_2$ or IV.

### 3.3. NADH oxidation by respirasome

Oxidation of NADH by respirasomes was recorded spectrophotometrically at 340 nm in the presence of cytochrome *c* and DBQ (Fig. 3). NADH dehydrogenase activity of respirasomes was inhibited by rotenone (Fig. 3A) demonstrating that this activity belongs exclusively to complex I and alternative NADH dehydrogenases were absent. Interestingly, reduction of DBQ by complex I was stopped when complex $III_2$ and complex IV were inhibited by antimycin A or cyanide, respectively, even in the presence of an excess of coenzyme Q and cytochrome *c* (Fig. 3B and C). Inhibition of the NADH:DBQ oxidoreductase activity occurs even if inhibitor (*i.e.* Antimycin A or cyanide) was added before NADH (Fig. 3B and C). This observation indicates that activity of complex I is tightly coordinated with the activities of complexes $III_2$ and IV in the respirasome (Fig. 2). Antimycin A and cyanide have no effect on free-complex I activity (Fig. 3E and F). Remarkably, the ratio between NADH oxidation (*i.e.* 959 ± 197 nmol NADH oxidize/mg of CI·min; see Fig. 3) and oxygen reduction (*i.e.* 397 ± 81 nmol $O_2$ reduced/mg of CI·min, see Fig. 2) by respirasomes was 2.42 ± 0.3, very close to the theoretical value of 2 for the electron

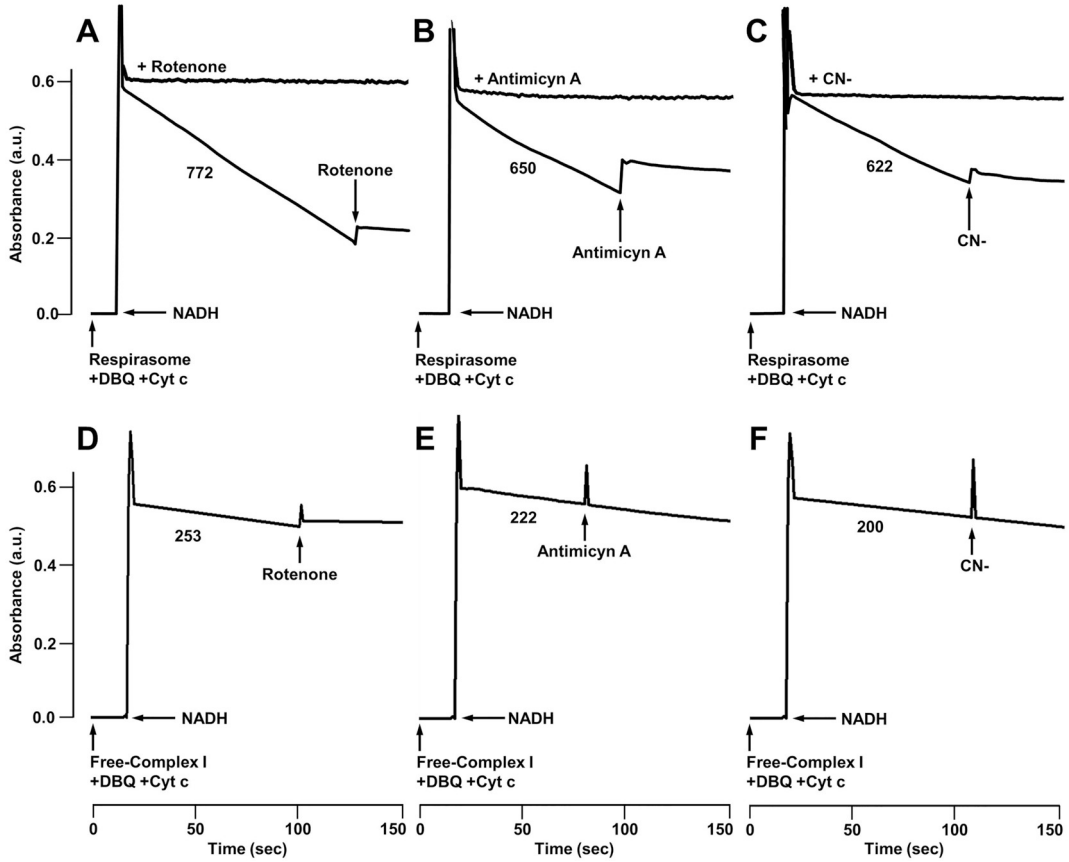


**Fig. 3.** Effect of rotenone, antimycin A and cyanide on NADH:DBQ oxidoreductase activity of respirasome. Respirasomes were incubated in the buffer described in Fig. 2. NADH oxidation was monitored by NADH absorbance at 340 nm. Where is indicated respirasome, DBQ (65 μM), cytochrome *c* (60 μg/ml), NADH (150 nmol), and (A) rotenone (15 μM), (B) antimycin A (5 μg/ml), or (C) cyanide (3 mM), were added. Addition of inhibitor before NADH is showed as +Rotenone (A), +Antimycin A (B), or +CN- (C). Activity of free-complex I was assayed in similar conditions in the presence of rotenone (D), antimycin A (E) or cyanide (F). The number below each recording represents the velocity of NADH oxidation. The mean ± S.D. value of NADH:DBQ oxidoreductase activity for respirasome in this experimental condition was 959 ± 197 nmol NADH oxidize/mg of CI·min (n = 9). Results were obtained from 7 different preparations.

flux from NADH to oxygen through respiratory complexes I-$III_2$-IV.

Oxygen uptake stimulation by the addition of DBQ and cytochrome *c* (Fig. 2A and B) suggests that mobile electron carriers were taken from the medium, and their microdiffusion between complexes could play an important role in electron flux. Interestingly, inhibition of complexes $III_2$ or IV stops the NADH:DBQ oxidoreductase activity of the respirasome (Fig. 3), suggesting that protein-protein contacts between complexes I, $III_2$ and IV could play an important role in the regulation of respirasome activity. In this sense, we have previously characterized the role of protein-protein interactions in the activity of the complex V dimer [36]. Then, the characterization of NADH dehydrogenase activity in respirasomes and free-complex I could be helpful to elucidate the role of the interactions between complexes in the respirasomes.

### 3.4. NADH dehydrogenase activity from complex I versus NADH dehydrogenase activity from respirasome

As a first step, activity of NADH:DBQ oxidoreductase from respirasome and free-complex I was determined following the change in absorbance at 340 nm.

Activity of NADH:DBQ oxidoreductase by respirasome (Fig. 4A and B) or free-complex I (Fig. 4C and D) increased as the NADH or DBQ concentrations were raised. The data were fitted to the Michaelis-Menten equation. Respirasome showed a $V_{max}$ = 3340 ± 150 nmol NADH oxidized·(mg of CI·min)$^{-1}$, a $K_{M\text{-}NADH}$ = 19 ± 4 μM and a $K_{M\text{-}DBQ}$ = 76 ± 15 μM. In contrast, free-complex I showed a $V_{max}$ value of 1000 ± 80 nmol NADH oxidized·(mg of CI·min)$^{-1}$, a $K_{M\text{-}NADH}$ = 50 ± 11 μM and a $K_{M\text{-}DBQ}$ = 103 ± 30 μM (Table 2). It has been reported that phospholipid reconstitution could increase the activity of DDM-isolated complex I from *Yarrowia lipolytica* [47]; however, this effect was not observed in the free-complex I or respirasome from *U. maydis* (see Suppl material). The Lineweaver-Burk plot for free-complex I as well as complex I from respirasome was consistent with a random Bi Bi mechanism, which predicts a ternary complex (*i.e.* NADH-CI-DBQ).

The $k_{cat}$ values for free-complex I and respirasome were 15 ± 1 $s^{-1}$ and 49 ± 2 $s^{-1}$, respectively (Table 2), confirming that respirasome is 3-times more active than free-complex I. Additionally, the $k_{cat}/K_{M\text{-}NADH}$ values of free-complex I and respirasome were 2.9 × $10^5$ ± 0.2 × $10^5$ and 2.6 × $10^6$ ± 0.6 × $10^6$ $M^{-1}$ $s^{-1}$, respectively; while the $k_{cat}/K_{M\text{-}DBQ}$ values were 1.4 × $10^5$ ± 0.3 × $10^5$ and 6.5 × $10^5$ ± 1.3 × $10^5$ $M^{-1}$ $s^{-1}$ for free-complex I and respirasome, respectively (Table 2), indicating a higher specificity of respirasome for NADH and DBQ. These results indicate that incorporation of complex I into respirasomes and the interaction between complexes I, $III_2$ and IV, has a stimulatory effect on the activity and affinity of complex I.

### 3.5. Proteins associated to respirasomes

The MS/MS analysis of isolated respirasomes showed five proteins related with the organization of mitochondrial architecture: Prohibitins 1 (UMAG_11092) and 2 (UMAG_05030); Fcj1 (UMAG_00635), Rcf2 (UMAG_03929) and the mitochondrial inner membrane organizing system protein 1 (UMAG_10488). All these proteins showed

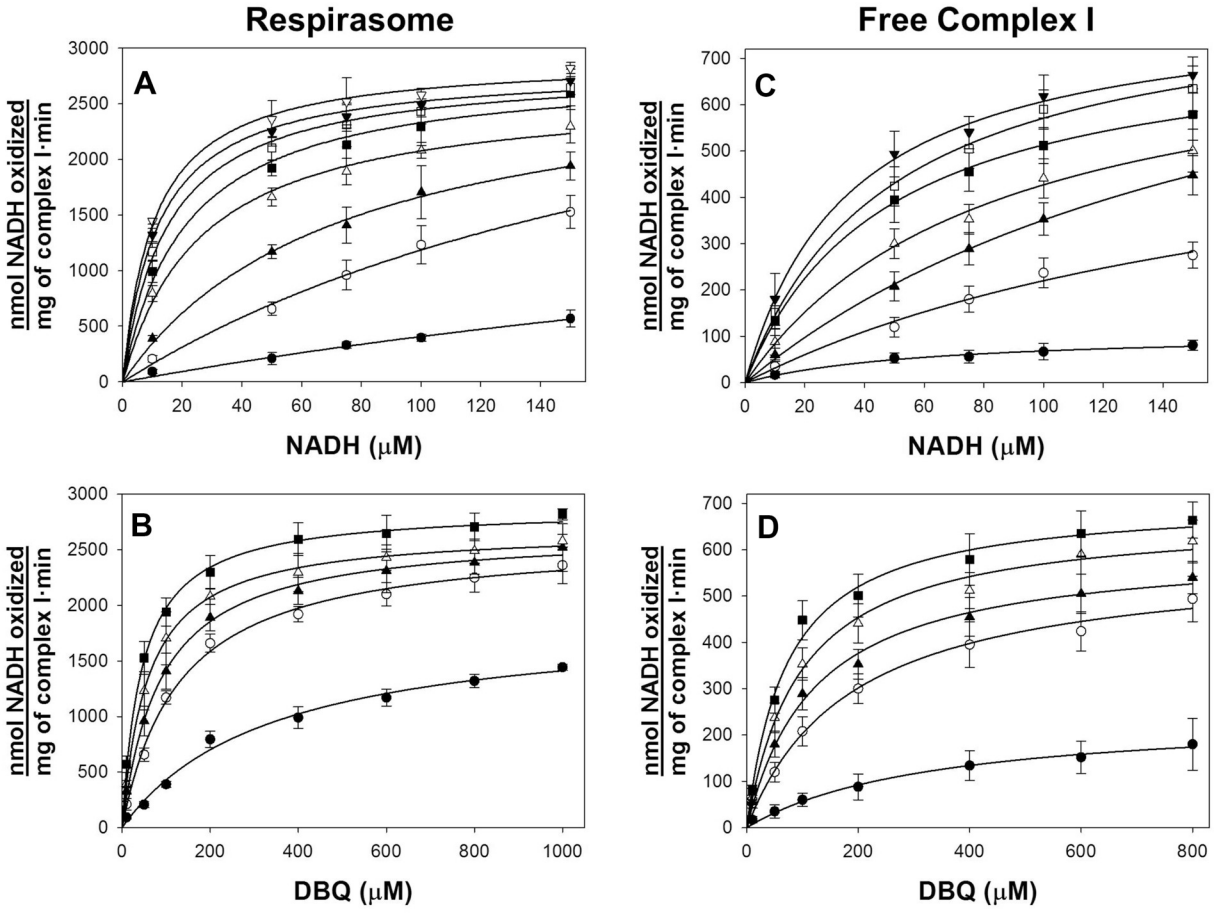


**Fig. 4.** Kinetic characterization of NADH:DBQ activity from respirasome and free-complex I. The dependence of respirasome (A) and free-complex I (C) activity on NADH at different fixed concentrations of DBQ, and dependence of respirasome (B) and free-complex I (D) activity on DBQ at different fixed NADH concentrations, were fitted to the Michaelis-Menten equation. In (A) and (C) the fixed concentration of DBQ was (●) = 10; (○) = 50; (▲) = 100; (Δ) = 200; (■) = 400; (□) = 600; (▼) = 800; and (▽) = 1000 μM. In (B) and (D) the fixed concentration of NADH was (●) = 10; (○) = 50; (▲) = 75; (Δ) = 100; and (■) = 150 μM. The data are the average of four replicates from five independent preparations. The activity was corrected by complex I amount in each preparation of respirasomes and free-complex I as described in Materials and methods section. Error bars represent S.D.

**Table 2**
Kinetics parameters of NADH:DBQ oxide-reductase activity of the respirasome and the free-complex I from *Ustilago maydis* mitochondria.

| | Free-complex I[a] | Respirasome[a] |
|---|---|---|
| $V_{max}$ (nmol NADH oxidized/ mg complex I·min$^{-1}$) | 1000 ± 80 | 3340 ± 150 |
| $k_{cat}$ ($s^{-1}$) | 15 ± 1 | 49 ± 2 |
| | NADH | |
| $K_M$ (μM) | 50 ± 11 | 19 ± 4 |
| $k_{cat}/K_m$ ($M^{-1}\,s^{-1}$) | $2.9 \times 10^5 \pm 0.2 \times 10^5$ | $2.6 \times 10^6 \pm 0.6 \times 10^6$ |
| | DBQ | |
| $K_M$ (μM) | 103 ± 30 | 76 ± 15 |
| $k_{cat}/K_m$ ($M^{-1}\,s^{-1}$) | $1.4 \times 10^5 \pm 0.3 \times 10^5$ | $6.5 \times 10^5 \pm 1.3 \times 10^5$ |

[a] Complex I mol in free-Complex I and respirasome samples was determined as described in Materials and methods section, and kinetics parameters were showed as mg of Complex I.

transmembrane domains but only prohibitin 2 and Rcf2 presented a glycine zipper motif in the transmembrane domains. It has been suggested that proteins with transmembrane glycine zippers play a structural role as glue between the membrane proteins [51]. Finally, three proteins with the pentatricopeptide repeat domain (PPR domain: UMAG_06347 and UMAG_11282; PET127: UMAG_02275) were associated with the respirasome sample.

## 4. Discussion

Mitochondrial respiratory complex I, $III_2$ and IV are membrane proton-pumps that transform the energy of NADH into the proton electrochemical gradient ($\Delta\mu_{H+}$) across the inner membrane. The free energy stored in the $\Delta\mu_{H+}$ is utilized for ATP synthesis. Actually, stable interactions between the respiratory complexes have been determined, and these new structures are named supercomplexes. Although composition and stoichiometry of supercomplexes are diverse, if complexes I, $III_2$ and IV are presents, the electron flow could occur from NADH to oxygen (*i.e.* a respirasome). The respirasome has been described in mitochondria from different eukaryotes such as bovine [16], *Neurospora crassa* [12], and prokaryotes as the α-proteobacteria *Paracoccus denitrificans* [9].

In this work the *U. maydis* respirasome was efficiently solubilized with digitonine and isolated as a highly stable unit (Fig. 1). Composition of *U. maydis* respirasome was assessed by MS/MS analysis (Table 1), in-gel activity (*i.e.* complex I and IV), and NADH:$O_2$ oxidoreductase activity (*i.e.* electron flux from NADH to oxygen). The minimal stoichiometry of the respirasome was $I_1III_2IV_1$ with an apparent molecular mass of 1630 kDa (Fig. 1).

Oxygen consumption supported by NADH oxidation strongly indicates that cytochrome *c* and coenzyme Q were present in isolated *U. maydis* respirasome (Fig. 2A), similar to that described for the respirasome obtained from bovine heart mitochondria [52]. This could be

possible because the binding of cytochrome *c* to complex $III_2$ is strong [53,54], and coenzyme Q was embedded in the lipid annulus of the respirasome. However, incorporation of fresh cytochrome *c* and DBQ into isolated respirasomes increased the electron flow from NADH to oxygen, suggesting that the respirasome can take the quinone and cytochrome *c* from the medium.

Recent experimental evidences support that substrate channeling inside the respirasome doesn't occur. Electron microscopy showed that each monomer in complex III dimer ($III_2$) contains two Q binding sites ($Q_P$ and $Q_N$), which are located on opposite sides of the dimer. The activity of complex $III_2$ involves oxidation of $QH_2$ and reduction of cytochrome *c*, in a process called the Q-cycle. $QH_2$ binds at the $Q_P$ site and its electrons are transferred, one to cytochrome *c* in the intermembrane space *via* the Rieske protein, and the other to a Q bound at the $Q_N$ site, generating a semiquinone ($Q\cdot$). A new $QH_2$ binds at the $Q_P$ site and a second cytochrome *c* is reduced, and the $Q\cdot$ bound at the $Q_N$ site is fully reduced to $QH_2$, which is released into the ubiquinone pool. Kinetic analysis has demonstrated the alternating activity of each monomer [55].

The cryo-electron microscopy analysis of the respirasome shows that the Q binding site of one monomer of complex $III_2$ is facing the Q site of complex I but separated by ~10 nm (~100 Å), while the other monomer is facing complex IV [18]. Also, these studies showed that there were no proteins involved in substrate channeling between the Q sites of complex I and complex $III_2$ [18].

Indeed, a time-resolved kinetic study of the respiratory chain in submitochondrial particles or mitochondrial membranes showed that Q exists as a single, common pool which is exchanged freely between respiratory complexes, including supercomplexes [56]. An elegant approach to test the electron channeling in the respirasome was provided by Fedor and Hirst [20], who hypothesized that in the presence of electron channeling between complexes I and $III_2$, the respiratory activity supported by NADH should be insensitive to enzymes that take the $QH_2$ from the quinone pool. Using a cyanide-insensitive, non-electrogenic quinol oxidase (AOX), they probed that adding AOX to bovine submitochondrial particles the NADH oxidation rate increases and becomes cyanide insensitive. They concluded that channeling doesn't occur because quinol produced by complex I is released into the quinone pool and oxidized by AOX [20].

However, a recent report shows that in the inner mitochondrial membrane complex I is heterogeneously distributed [57]. In bovine heart about 44% of complex I occurs as a single copy ($I_1$); 16% as $I_1III_2$ supercomplexes, and 40% as $I_1III_2IV_{1-2}$ respirasome [57]. In *Yarrowia lipolytica* the arrangements of complex I founded were: complex I by itself (40%); supercomplexes $I_1$:$III_2$ (13%); and $I_1III_2IV_{1-2}$ (47%) [57].

In this sense, the kinetic behavior of complex I in the different supercomplexes found in the membrane is not necessarily the same. An approach to determine the properties of respirasome is to isolate it. Interestingly, although the NADH:$O_2$ oxidoreductase activity of *U. maydis* respirasome was sensitive to classical respiratory inhibitors (Fig. 2), inhibition of complexes $III_2$ or IV prevented NADH oxidation (Fig. 3) in the presence of an excess of DBQ and cytochrome *c*. Particularly, inhibition of NADH:DBQ oxidoreductase activity by antimycin A or cyanide strongly supports the idea that interactions between complex I and complexes $III_2$ and IV might regulate the activity of complex I, and therefore the respirasome activity. In line with this hypothesis, inhibition of NADH:$O_2$ oxidoreductase activity in the respirasome with antimycin A or cyanide does not induce $H_2O_2$ or superoxide production, as confirmed by catalase addition (Fig. 2) or Amplex Red assay in the presence or absence of superoxide dismutase. Since complex IV doesn't use the product of complex I, and its active site is ~20 nm away from complex I Q site [18], the cross-talk (*i.e.* complex-complex contacts) between complexes IV and I is a working hypothesis to explain that inhibition of complex IV induces the inhibition of complex I.

It has been described that intersubunit contacts play a significant role in the catalytic properties of many enzymes. Particularly, in the 3-deoxy-*d*-manno-octulosonate-8-P synthase the subunit interphase is important for substrate selectivity and binding [58]; and in the glucosamine-6-P deaminase from *Escherichia coli* the contacts between the subunits modify the allosteric equilibrium between the R and T-state [59]. In *U. maydis* the contacts between monomers in the dimer of $F_1F_0$-ATP synthase increase the ATPase activity and decrease the $IC_{50}$ for oligomycin [36].

In the respirasome, interactions between complex IV and complex I involve subunit 7A of complex IV and either ND5 or the 39-kDa subunit of complex I. Additionally, complexes IV and $III_2$ interact through subunits cox 7A and cox 8B and regions of subunits QCR9, QCR8 of complexes IV and $III_2$, respectively [57].

To explore the effect of complex-complex contacts in the respirasome, we decided to determine NADH:DBQ oxidoreductase activity of complex I in two states, free as well as incorporated in the respirasome. Free-complex I from *U. maydis* showed a $V_{max}$ of 1000 ± 80 nmol NADH oxidized·(mg of complex I·min)$^{-1}$; similar values (420–840 nmol NADH·(mg·min)$^{-1}$) have been reported for *Yarrowia lipolitica* [44,60]. However, kinetic analysis showed that the activity of *U. maydis* respirasomal complex I was 3-time higher than that of the individual complex I ($V_{max}$ = 3340 ± 150 nmol NADH oxidized·(mg of complex I·min)$^{-1}$), and the affinity for NADH and DBQ was also higher. These observations indicate that incorporation of complex I in supercomplexes (*i.e.* respirasome) increased their catalytic ($k_{cat}$) and the specificity ($k_{cat}/K_M$) constants, illustrating the possible role of the tight interactions between complexes I, $III_2$ and IV. In contrast with our results, the group of Shinzawa-Itoh described that the supercomplexes isolated from bovine heart mitochondria showed an NADH:$Q_1$ oxidoreductase activity of 700–1120 nmol NADH·(mg of SC·min)$^{-1}$ in the presence of 150 μM NADH, 37 μM $Q_1$, 200 μM cytochrome *c* and 2 mM KCN [61]. The activity of *U. maydis* respirasome was 3-time higher than the activity of bovine supercomplexes, and under similar concentrations of NADH, coenzyme Q, and cytochrome *c* the *U. maydis* respirasome showed only 30% of its $V_{max}$ (Fig. 4). It's important to note that KCN was present in the mixture assay of the bovine supercomplexes activity [61], while KCN had a different effect on *U. maydis* respirasome.

An important difference between bovine and *U. maydis* respirasomes is the dependence of complex I activity on active complexes $III_2$ and IV. Here we showed that NADH:DBQ oxidoreductase activity of complex I was depended on active complex $III_2$ and IV, even in the presence of an excess of DBQ and cytochrome *c*; moreover, inhibition of complex IV abolished complex I activity (Fig. 3). Bovine respirasome showed similar behavior only if coenzyme Q concentration was limiting, suggesting that activities of complex $III_2$ and IV were important to remove the products [61]. Under this condition electron leak at mammalian complex I or contribution to $QH_2$ pool would be probable [61]. Additionally, complex-complex contacts in *U. maydis* respirasome promotes NADH:DBQ activity, while in bovine respirasome this stimulating effect was not observed.

To explain the effect of cyanide or antimycin A on the activity of complex I in respirasome, we hypothesized that the respirasome in *U. maydis* is “tighter”, and the interactions between the complexes promoted a conformational change in complex I (*i.e.* formation of deactive status of complex I). Studies on the deactive state of complex I, which is formed during ischemia, showed that an unstructured region in the loop of ND3 prevents coenzyme Q binding [62]. Actually, this deactive state is considered a regulatory mechanism of complex I to minimize ischemia-reperfusion injury [63]. Thus, although a deactive state of complex I in *U. maydis* must be determined experimentally, in the respirasome the cyanide inhibition of complex IV could recreate the ischemia condition, promoting the “deactive state” of complex I and preventing NADH oxidation and coenzyme Q reduction.

Regarding the identity of proteins associated whit the *U. maydis*

respirasomes sample, prohibitins 1 and 2 [64,65] and Rcf2 [66,67] have an important role in the formation and stabilization of supercomplexes. Although Fcj1 has a role in the formation of the mitochondrial crista [68], it has not been reported a role of this protein in respirasome formation.

The common features of the pentatricopeptide repeat domain proteins and Pet127 detected in the respirasome sample are the mitochondrial localization and mRNA binding during the synthesis of proteins in mitochondria. Although deletion of some members of these proteins results in a complete loss of mitochondrial respiratory capacity [69,70], their precise role in the *U. maydis* respirasome should be experimentally determined.

Under physiological conditions, the interaction between complexes I-$III_2$-IV in the respirasome may have two possible roles: 1) stimulate the NADH:DBQ oxidoreductase activity of complex I, and 2) provide a mechanism of regulation of complex I, stabilizing its deactive/active status to prevent ROS production. If cellular ATP decreases, individual mitochondrial respiratory complexes could associate into respirasomes to improve the electron flux, the proton pumping and generate the $\Delta\mu_{H+}$ needed for ATP synthesis. Contrary, if there is not a cellular demand for ATP (or an ischemic state) complex I can be in a deactive state to decrease NADH consumption and cytochrome *c* reduction, and then drop the electron flux reducing the ROS production.

## Author contribution

Reyes-Galindo M, Suarez R and Flores-Herrera O designed and performed principal experiments; Esparza-Perusquía M, respirasomes isolation and technical assistance; de Lira-Sánchez J, ROS production analysis and technical assistance; Pardo JP and Martínez F analyzed data; Flores-Herrera O supervised project and wrote the paper with contributions from all authors.

## Transparency document

The Transparency document associated with this article can be found, in online version.

## Declaration of Competing Interest

The authors declare no conflict of interest.

## Acknowledgments

We dedicate this work as a memorial to Professor PhD. Edmundo Chávez-Cossío, an exceptional friend and colleague, who passed away suddenly on December 24, 2018. This work was supported by Dirección General de Asuntos del Personal Académico (DGAPA) (IN222617, IN222117 and IN211715) from Universidad Nacional Autónoma de México (UNAM) and Consejo Nacional de Ciencia y Tecnología (CONACyT) (168025 and 254904). MR-G is a student of Facultad de Medicina (309210120) from UNAM and fellowship from Programa de Apoyo y Fomento a la Investigación Estudiantil (AFINES); RS is a student of Ingeniería Bioquímica (11120199) from Instituto Tecnológico de Morelia, México; ME-P is a PhD student of the Programa de Doctorado en Ciencias Biológicas (511021118) from UNAM and supported by the CONACyT through a doctoral scholarship (254400). JdL-S is a PhD student of the Programa de Doctorado en Ciencias Biomédicas (518024299) from UNAM and supported by the CONACyT through a doctoral scholarship (666472). The authors thank to the Posgrado en Ciencias Biológicas and Ciencias Biomédicas from UNAM for the academic support.

## Appendix A. Supplementary data

Supplementary data to this article can be found online at https://doi.org/10.1016/j.bbabio.2019.06.017.

## References

[1] P. Mitchell, Coupling of photophosphorylation to electron and hydrogen transfer by a chemiosmotic type of mechanism, Nature. 191 (1961) 144–148.
[2] P. Mitchell, Chemiosmotic Coupling and Energy Transduction, Glynn Research, LTD., Bodmin, Cornwall, U.K, 1968, pp. 1–111.
[3] P. Mitchell, Chemiosmotic coupling in oxidative and phosphosynthetic phosphorylation, Biochim. Biophys. Acta 1807 (2011) 1507–1538.
[4] D.G. Nicholls, S.J. Ferguson, Bioenergetics 4. London, Academic Press, 2013.
[5] C.R. Hackenbrock, B. Chazotte, S.S. Gupte, The random collision model and a critical assessment of diffusion and collision in mitochondrial electron transport, J. Bioenerg. Biomembr. 18 (1986) 331–368.
[6] J. Vonck, E. Schäfer, Supramolecular organization of protein complexes in the mitochondrial inner membrane, Biochim. Biophys. Acta 1793 (2009) 117–124.
[7] R. Acín-Perez, J.A. Enriquez, The function of the respiratory supercomplexes: the plasticity model, Biochim. Biophys. Acta 1837 (2014) 444–450.
[8] E.A. Berry, B.L. Trumpower, Isolation of ubiquinol oxidase from *Paracoccus denitricans* and resolution into cytochrome bc1 and cytochrome c-aa3 complexes, J. Biol. Chem. 260 (1985) 2458–2467.
[9] A. Stroh, O. Anderka, K. Pfeiffer, T. Yagi, M. Finel, B. Ludwig, H. Schagger, Assembly of respiratory complexes I, III, and IV into NADH oxidase supercomplex stabilizes complex I in *Paracoccus denitrificans*, J. Biol. Chem. 279 (2004) 5000–5007.
[10] H. Schägger, K. Pfeiffer, Supercomplexes in the respiratory chains of yeast and mammalian mitochondria, EMBO J. 19 (2000) 1777–1783.
[11] R.A. Stuart, Supercomplex organization of the oxidative phosphorylation enzymes in yeast mitochondria, J. Bioenerg. Biomembr. 40 (2008) 411–417.
[12] I. Marques, N.A. Dencher, A. Videira, F. Krause, Supramolecular organization of the respiratory chain in *Neurospora crassa* mitochondria, Eukaryot. Cell 6 (2007) 2391–2405.
[13] H. Eubel, L. Jänsch, H.P. Braun, New insights into the respiratory chain of plant mitochondria. Supercomplexes and a unique composition of complex II, Plant Physiol. 133 (2003) 274–286.
[14] H. Eubel, J. Heinemeyer, H.P. Braun, Identification and characterization of respirasomes in potato mitochondria, Plant Physiol. 134 (2004) 1450–1459.
[15] N.V. Dudkina, J. Heinemeyer, S. Sunderhaus, E.J. Boekema, H.P. Braun, Respiratory chain supercomplexes in the plant mitochondrial membrane, Trends Plant Sci. 11 (2006) 232–240.
[16] H. Schägger, K. Pfeiffer, The ratio of oxidative phosphorylation complexes I–V in bovine heart mitochondria and the composition of respiratory chain supercomplexes, J. Biol. Chem. 276 (2001) 37861–37867.
[17] G. Jinke, W. Meng, G. Runyu, Y. Kaige, L. Jianlin, G. Ning, Y. Maojun, The architecture of the mammalian respirasome, Nature. 537 (2016) 639–643.
[18] J.A. Letts, K. Fiedorczuk, L.A. Sazanov, The architecture of respiratory supercomplexes, Nature. 537 (2016) 644–648.
[19] M.L. Genova, A. Baracca, A. Biondi, G. Casalena, M. Faccioli, A.I. Falasca, G. Formiggini, G. Sgarbi, G. Solaini, G. Lenaz, Is supercomplex organization of the respiratory chain required for optimal electron transfer activity? Biochim. Biophys. Acta 1777 (2008) 740–746.
[20] J.G. Fedor, J. Hirst, Mitochondrial supercomplexes do not enhance catalysis by quinone channeling, Cell Metab. 28 (2018) 525–531.
[21] R. Acin-Perez, M.P. Bayona-Bafaluy, P. Fernandez-Silva, R. Moreno-Loshuertos, A. Perez-Martos, C. Bruno, C.T. Morales, J.A. Enriquez, Respiratory complex III is required to maintain complex I in mammalian mitochondria, Mol. Cell 13 (2004) 805–815.
[22] F. Diaz, H. Fukui, S. Garcia, C.T. Moraes, Cytochrome c oxidase is required for the assembly/stability of respiratory complex I in mouse fibroblasts, Mol. Cell. Biol. 26 (2006) 4872–4881.
[23] Y.C. Chen, E.B. Taylor, N. Dephoure, J.M. Heo, A. Tonhato, I. Papandreou, N. Nath, N.C. Denko, S.P. Gygi, J. Rutter, Identification of a protein mediating respiratory supercomplex stability, Cell Metab. 15 (2012) 348–360.
[24] E. Maranzana, G. Barbero, A.I. Falasca, G. Lenaz, M.L. Genova, Mitochondrial respiratory supercomplex association limits production of reactive oxygen species from complex I, Antioxid. Redox Signal. 19 (2013) 1469–1480.
[25] E. Lapuente-Brun, R. Moreno-Loshuertos, R. Acín-Pérez, A. Latorre-Pellicer, C. Colás, E. Balsa, E. Perales-Clemente, P.M. Quirós, E. Calvo, M.A. Rodríguez-Hernández, P. Navas, R. Cruz, Á. Carracedo, C. López-Otín, A. Pérez-Martos, P. Fernández-Silva, E. Fernández-Vizarra, J.A. Enríquez, Supercomplex assembly determines electron flux in the mitochondrial electron transport chain, Science. 340 (2013) 1567–1570.
[26] K. Ikeda, S. Shiba, K. Horie-Inoue, K. Shimokata, S. Inoue, A stabilizing factor for mitochondrial respiratory supercomplex assembly regulates energy metabolism in muscle, Nat. Commun. 4 (2013) 2147–2156.
[27] M.L. Genova, G. Lenaz, Functional role of mitochondrial respiratory supercomplexes, Biochim. Biophys. Acta 1837 (2014) 427–443.
[28] Y. Chaban, E.J. Boekema, N.V. Dudkina, Structures of mitochondrial oxidative phosphorylation supercomplexes and mechanisms for their stabilization, Biochim. Biophys. Acta 1837 (2014) 418–426.
[29] M.P. McCann, K.M. Snetselaar, A genome-based analysis of amino acid metabolism in the biotrophic plant pathogen *Ustilago maydis*, Fungal Genet. Biol. 45 (Suppl. 1) (2008) S77–S87.
[30] J. Ruiz-Herrera, C.G. León, L. Guevara-Olvera, A. Cárabez-Trejo, A yeast-mycelial dimorphism of haploid and diploid strains of *Ustilago maydis* in liquid culture,

Microbiology. 1421 (1995) 695–703.
[31] O. Juárez, G. Guerra, F. Martínez, J.P. Pardo, The mitochondrial respiratory chain of *Ustilago maydis*, Biochim. Biophys. Acta 1658 (2004) 244–251.
[32] W.F. Waterfield, H.D. Sisler, A convenient procedure for rapid release of protoplasts from *Ustilago maydis*, Biotechniques. 6 (1988) 832–834.
[33] H. Schägger, W.A. Cramer, G. von Jagow, Analysis of molecular masses and oligomeric states of protein complexes by blue native electrophoresis and isolation of membrane protein complexes by two-dimensional native electrophoresis, Anal. Biochem. 217 (1994) 220–230.
[34] C. Jung, C.M. Higgins, Z. Xu, Measuring the quantity and activity of mitochondrial electron transport chain complexes in tissues of central nervous system using blue native polyacrylamide gel electrophoresis, Anal. Biochem. 286 (2000) 214–223.
[35] I. Wittig, M. Karas, H. Schägger, High resolution clear native electrophoresis for in-gel functional assays and fluorescence studies of membrane protein complexes, Mol. Cell. Proteomics 6 (2007) 1215–1225.
[36] M. Esparza-Perusquia, S. Olvera-Sanchez, J.P. Pardo, G. Mendoza-Hernandez, F. Martinez, O. Flores-Herrera, Structural and kinetics characterization of the $F_1F_0$-ATP synthase dimer. New repercussion of monomer-monomer contact, Biochim. Biophys. Acta Bioenerg. 1858 (2017) 975–981.
[37] D. De los Ríos-Castillo, M. Zarco-Zavala, S. Olvera-Sanchez, J.P. Pardo, O. Juarez, F. Martinez, G. Mendoza-Hernandez, J.J. García-Trejo, O. Flores-Herrera, Atypical cristae morphology of human syncytiotrophoblast mitochondria: role for complex V, J. Biol. Chem. 286 (2011) 23911–23919.
[38] K.M.C. Sinjorgo, T.B.M. Hakvoort, I. Durak, J.W. Draijer, J.K.P. Post, A.O. Muijsers, Human cytochrome c oxidase isoenzymes from heart and skeletal muscle: purification and properties, Biochim. Biophys. Acta 850 (1987) 144–150.
[39] Y. Nakashima, K. Shinzawa-Itoh, K. Watanabe, K. Naoki, N. Hano, S. Yoshikawa, Steady-state kinetics of NADH:coenzyme Q oxidoreductase isolated from bovine heart mitochondria, J. Bioenerg. Biomembr. 34 (2002) 11–19.
[40] A.D. Vinogradov, V.G. Grivennikova, Generation of superoxide-radical by the NADH:ubiquinone oxidoreductase of heart mitochondria, Biochemistry (Mosc) 70 (2005) 120–127.
[41] S. Dröse, A. Galkin, U. Brandt, Proton pumping by complex I (NADH:ubiquinone oxidoreductase) from *Yarrowia lipolytica* reconstituted into proteoliposomes, Biochim. Biophys. Acta 1710 (2005) 87–95.
[42] M. Candela, E. Zaccherini, D. Zannoni, Respiratory electron transport and light-induced energy transduction in membranes from the aerobic photosynthetic bacterium *Roseobacter denitrificans*, Arch. Microbiol. 175 (2001) 168–177.
[43] A. Galkin, U. Brandt, Superoxide radical formation by pure complex I (NADH:ubiquinone oxidoreductase) from *Yarrowia lipolytica*, J. Biol. Chem. 280 (2005) 30129–30135.
[44] F.A. Rotsaert, M.G. Ding, B.L. Trumpower, Differential efficacy of inhibition of mitochondrial and bacterial cytochrome bc1 complexes by center N inhibitors antimycin, ilicicolin H and funiculosin, Biochim. Biophys. Acta 1777 (2008) 211–219.
[45] D. Guo, T. Nguyen, M. Ogbi, H. Tawfik, G. Ma, Q. Yu, R.W. Caldwell, J.A. Johnson, Protein kinase C-epsilon coimmunoprecipitates with cytochrome oxidase subunit IV and is associated with improved cytochrome-c oxidase activity and cardioprotection, Am. J. Physiol. Heart Circ. Physiol. 293 (2007) H2219–H2230.
[46] T. Sugio, M. Fujii, Y. Ninomiya, T. Kanao, A. Negishi, F. Takeuchi, Reduction of $Hg^{2+}$ with reduced mammalian cytochrome c by cytochrome c oxidase purified from a mercury-resistant *Acidithiobacillus ferrooxidans* strain, MON-1, Biosci. Biotechnol. Biochem. 72 (2008) 1756–1763.
[47] S. Dröse, K. Zwicker, U. Brandt, Full recovery of the NADH:ubiquinone activity of complex I (NADH:ubiquinone oxidoreductase) from *Yarrowia lipolytica* by the addition of phospholipids, Biochim. Biophys. Acta 1156 (2002) 65–72.
[48] A.I. Nesvizhskii, A. Keller, E. Kolker, R. Aebersold, A statistical model for identifying proteins by tandem mass spectrometry, Anal. Chem. 75 (2003) 4646–4658.
[49] M. Ashburner, C.A. Ball, J.A. Blake, D. Botstein, H. Butler, J.M. Cherry, A.P. Davis, K. Dolinski, S.S. Dwight, J.T. Eppig, M.A. Harris, D.P. Hill, L. Issel-Tarver, A. Kasarskis, S. Lewis, J.C. Matese, J.E. Richardson, M. Ringwald, G.M. Rubin, G. Sherlock, Gene ontology: tool for the unification of biology. The Gene Ontology Consortium, Nat. Genet. 25 (2000) 25–29.
[50] O.H. Lowry, N.J. Rosebrough, A.L. Rarr, R.J. Randall, Protein measurement with the Folin-phenol reagent, J. Biol. Chem. 193 (1951) 265–275.
[51] S. Kim, T.-J. Jeon, A. Oberai, D. Yang, J.J. Schmidt, J.U. Bowie, Transmembrane glycine zippers: physiological and pathological roles in membrane proteins, Proc. Natl. Acad. Sci. U. S. A. 102 (2005) 14278–14283.
[52] T. Althoff, D.J. Mills, J.-L. Popot, W. Kühlbrandt, Arrangement of electron transport chain components in bovine mitochondrial supercomplex $I_1III_2IV_1$, EMBO J. 30 (2011) 4652–4664.
[53] J. Heinemeyer, H.-P. Braun, E.J. Boekema, R. Kouril, A structural model of the cytochrome c reductase/oxidase supercomplex from yeast mitochondria, J. Biol. Chem. 282 (2007) 12240–12248.
[54] A. Nyola, C. Hunte, A structural analysis of the transient interaction between the cytochrome bc1 complex and its substrate cytochrome c, Biochem. Soc. Trans. 36 (2008) 981–985.
[55] M. Castellani, R. Covian, T. Kleinschroth, O. Anderka, B. Ludwig, B.L. Trumpower, Direct demonstration of half-of-the-sites reactivity in the dimeric cytochrome bc1 complex. Enzyme with one inactive monomer is fully active but unable to activate the second ubiquinol oxidation site in response to ligand binding at the ubiquinone reduction site, J. Biol. Chem. 285 (2010) 502–510.
[56] J.N. Blaza, R. Serreli, A.J.Y. Jones, K. Mohammed, J. Hirst, Kinetic evidence against partitioning of the ubiquinone pool and the catalytic relevance of respiratory-chain supercomplexes, Proc. Natl. Acad. Sci. U. S. A. 111 (2014) 15735–15740.
[57] K.M. Daviesa, T.B. Bluma, W. Kühlbrandt, Conserved in situ arrangement of complex I and III2 in mitochondrial respiratory chain supercomplexes of mammals, yeast, and plants, Proc. Natl. Acad. Sci. U. S. A. 115 (2018) 3024–3029.
[58] T.M. Allison, F.C. Cochrane, G.B. Jameson, E.J. Parker, Examining the role of intersubunit contacts in catalysis by 3-deoxy-d-manno-octulosonate 8-phosphate synthase, Biochemistry. 52 (2013) 4676–4686.
[59] D.A. Cisnerosa, G.M. Montero-Moran, S. Lara-Gonzalez, M.L. Calcagno, Inversion of the allosteric response of *Escherichia coli* glucosamine-6-P deaminase to N-acetylglucosamine 6-P, by single amino acid replacements, Arch. Biochem. Biophys. 421 (2004) 77–84.
[60] A. Waletko, K. Zwicker, A. Abdrakhmanova, V. Zickermann, U. Brandt, S. Kerscher, Histidine 129 in the 75-kDa subunit of mitochondrial complex I from *Yarrowia lipolytica* is not a ligand for [Fe4S4] cluster N5 but is required for catalytic activity, J. Biol. Chem. 280 (2005) 5622–5625.
[61] K. Shinzawa-Itoh, H. Shimomura, S. Yanagisawa, S. Shimada, R. Takahashi, M. Oosaki, T. Ogura, T. Tsukihara, Purification of active respiratory supercomplex from bovine heart mitochondria enables functional studies, J. Biol. Chem. 291 (2016) 4178–4184.
[62] J.N. Blaza, K.R. Vinothkumar, J. Hirst, Structure of the deactive state of mammalian respiratory complex I, Structure. 26 (2018) 312–319.
[63] E.T. Chouchani, V.R. Pell, E. Gaude, D. Aksentijevic, S.Y. Sundier, E.L. Robb, A. Logan, S.M. Nadtochiy, E.N.J. Ord, A.C. Smith, et al., Ischaemic accumulation of succinate controls reperfusion injury through mitochondrial ROS, Nature. 515 (2014) 431–435.
[64] L.G. Nijtmans, S.M. Artal, L.A. Grivell, P.J. Coates, The mitochondrial PHB complex: roles in mitochondrial respiratory complex assembly, ageing and degenerative disease, Cell. Mol. Life Sci. 59 (2002) 143–155.
[65] C. Jian, F. Xu, T. Hou, T. Sun, J. Li, H. Cheng, X. Wang, Deficiency of PHB complex impairs respiratory supercomplex formation and activates mitochondrial flashes, J. Cell Sci. 130 (2017) 2620–2630.
[66] V. Strogolova, A. Furness, M. Robb-McGrath, J. Garlich, R.A. Stuart, Rcf1 and Rcf2, members of the hypoxia-induced gene 1 protein family, are critical components of the mitochondrial cytochrome bc1-cytochrome c oxidase supercomplex, Mol. Cell. Biol. 32 (2012) 1363–1373.
[67] M. Vukotic, S. Oeljeklaus, S. Wiese, F.N. Vogtle, C. Meisinger, H.E. Meyer, A. Zieseniss, D.M. Katschinski, D.C. Jans, S. Jakobs, B. Warscheid, P. Rehling, M. Deckers, Rcf1 mediates cytochrome oxidase assembly and respirasome formation, revealing heterogeneity of the enzyme complex, Cell Metab. 15 (2012) 336–347.
[68] R. Rab, V. Soubannier, R. Scholz, F. Vogel, N. Mendl, A. Vasiljev-Neumeyer, C. Körner, R. Jagasia, T. Keil, W. Baumeister, M. Cyrklaff, W. Neupert, A.S. Reichert, Formation of cristae and crista junctions in mitochondria depends on antagonism between Fcj1 and Su e/g, J. Cell Biol. 185 (2009) 1047–1063.
[69] O. Puchta, M. Lubas, K.A. Lipinski, J. Piatkowski, M.M.P. Golik, DMR1 (CCM1/YGR150C) of *Saccharomyces cerevisiae* encodes an RNA-binding protein from the pentatricopeptide repeat family required for the maintenance of the mitochondrial 15S ribosomal RNA, Genetics. 184 (2010) 959–973.
[70] J.P. Mayorga, Y. Camacho-Villasana, M. Shingú-Vázquez, R. García-Villegas, A. Zamudio-Ochoa, A.E. García-Guerrero, G. Hernández, X. Pérez-Martínez, A novel function of Pet54 in regulation of cox1 synthesis in *Saccharomyces cerevisiae* mitochondria, J. Biol. Chem. 291 (2016) 9343–9355.